Plan for Safe Laser Beam Propagation from the Optical Communications Telescope Laboratory

K. E. Wilson,[1] W. T. Roberts,[1] V. Garkanian,[1] F. Battle,[2] R. Leblanc,[3] H. Hemmati,[1] and P. Robles[4]

JPL is building a state-of-the-art Optical Communications Telescope Laboratory (OCTL) to perform research and development of laser beam propagation and signal detection technologies to meet NASA's future needs for high-bandwidth communications from Earth-orbiting and deep-space probes. Laser beam propagation between ground and space is regulated by several government agencies—regulation that is significant when propagating high-brightness, Q-switched laser beams that will be used for uplinking commands to deep-space probes and as an acquisition, pointing, and tracking beacon for downlink optical communication. To ensure safe laser operation and beam propagation from the OCTL, JPL has identified a four-tier safety system. The safety system starts with safe beam propagation within the OCTL, extends to safe beam propagation through the air and into space, and is designed to meet the requirements of State (California Occupational Safety and Health Administration) and Federal agencies (Federal Aviation Administration and the U.S. Space Command's Laser Clearinghouse).

I. Introduction

With the decreasing availability of RF spectrum and the increasing demand for higher communications bandwidths, the terahertz laser communications bandwidths are seen as a viable augmentation of RF communications capability. Yet, cloud cover effects can impact link availability. Among the key strategies to increase availability and mitigate cloud cover effects is the global deployment of ground stations in atmospherically independent cells. Yet with such a deployment, one needs to address the impact of the uplink laser beams (the power densities on the communications downlink are usually eye safe) on the flying public and on space assets sensitive to laser radiation. Although the power densities of the uplink beacon required for Earth orbiters to track the ground station can, depending on mission, be within eye-safe laser levels, this will not be so when operations call for transmitting a beacon or commands to deep-space probes.

---

[1] Communications Systems and Research Section.

[2] Environmental Affairs Program.

[3] Occupational Safety Program.

[4] NASA Resident Office-JPL.

The research described in this publication was carried out by the Jet Propulsion Laboratory, California Institute of Technology, under a contract with the National Aeronautics and Space Administration.

As NASA aggressively pursues its solar system exploration strategy, an optical communications high-bandwidth link is seen as an attractive complement to X-band (∼7.2 to ∼8.5-GHz) and Ka-band (∼32 to ∼34.5-GHz) links. Current data-rate estimates are that several megabits per second will be needed to return the data from Mars probes [1]. With the higher-bandwidth and lower-power and lower-mass requirements promised by optical communications, JPL continues to investigate the challenges posed by this technology. We are building the Optical Communications Telescope Laboratory (OCTL) shown in Fig. 1 [2] to perform critical research in technology areas relevant to deep-space optical communications. In this article, we describe our plans to address the challenges of safe laser beam propagation from the OCTL into deep space. The thrust here is to develop techniques to support operations from a future network of remote unattended ground stations. The issues addressed cover safety of the operator, of the flying public, and of sensitive sensors onboard Earth-orbiting spacecraft.

To facilitate addressing the requirements of the various regulatory agencies, we have separated the safety zones into internal and external areas, with the zone internal to the laboratory, designated as Tier 0, controlled by California Occupational Safety and Health Administration (Cal-OSHA) guidelines. Over U.S. territories, the external zone is regulated by the Federal Aviation Administration (FAA) and the U.S. Space Command. We have divided this external zone into the three tiers shown in Fig. 2. Tiers 1 and 2

Fig. 1. JPL's Optical Communications Telescope Laboratory is located on Table Mountain in Wrightwood, California. The laboratory stands at a 2.2-km altitude and will house a 1-m telescope.

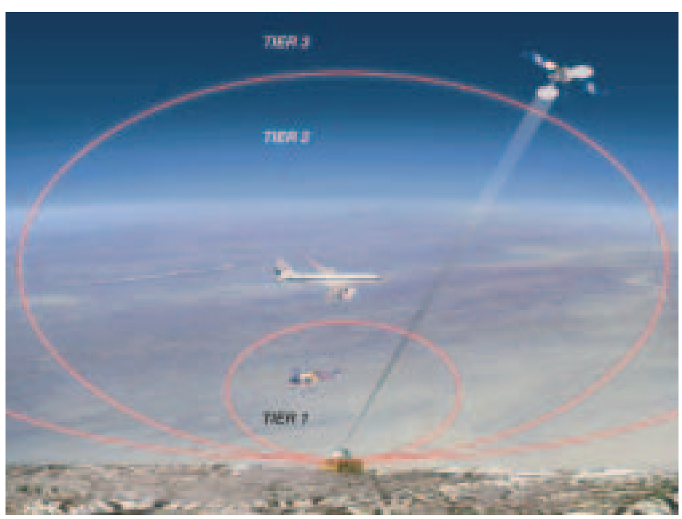

Fig. 2. JPL-defined safety and coordination levels for laser beam propagation into space.

are under FAA regulation, and the safety approach is designed to ensure the safety of the flying public. The approach uses a combination of radar and optical techniques to detect aircraft operating in FAA-controlled airspace. Tier 1 extends from the telescope dome out to a radius of 3.3 km (2 miles), and Tier 2 uses radar and extends to the edge of the commercial air corridor. Tier 1 provides the needed detection capability for aircraft flying close to the mountainous terrain around the Table Mountain Facility (TMF) that may be lost in the background clutter of the Tier-2 radar return.

Two approaches for the Tier-2 radar system are investigated. The first uses a radar feed provided to the OCTL by the FAA. The second uses on-site radar. This latter approach is especially applicable to ground stations deployed in remote sites of the world not covered by FAA radar. The third region, Tier 3, is regulated by the U.S. Space Command at Cheyenne Mountain. It extends from near-Earth to the ranges of geo-stationary and high-elliptical orbiting satellites.

In this article, we detail the systems that are being implemented to ensure safe propagation of high-power laser radiation from the JPL OCTL into space. In Section II, we describe the Tier-0 plans for safe laser beam propagation inside the facility that meet Cal-OSHA requirements. In Section III, we describe the plans for safe laser beam propagation through Tier 1, a 0.3- to 4-km-radius zone around the telescope. Tier 2, described in Section IV, is an ellipsoidal region around the telescope that extends to 20 km at zenith and out to 58 km at 20-deg elevation. The Tier-2 aircraft-avoidance approach adopted at the U.S. Air Force's Maui Optical Station (AMOS) uses the remote aircraft monitoring system developed by Boeing Technical Services (BTS). This system uses the radar feed from the FAA to display the location of aircraft relative to the optical ground-station location. Section V describes the safety strategies for the Tier-3 region that is under the cognizance of the U.S. Space Command's Laser Clearinghouse.

II. Cal-OSHA Safety Plans

In Tier 0, the safety of personnel working with lasers at the OCTL falls under the jurisdiction of Cal-OSHA. As a research facility, the OCTL will use a variety of lasers across a wide spectral range. While the selection of laser wavelengths will be driven primarily by the laser communications projects, work at OCTL will also include research and development to characterize the wavelength dependence of atmospheric turbulence on beam propagation. The lasers that will be used in experiments at the OCTL, along with their characteristics, are given in Table 1. The lasers in Table 1 are all designated American National Standards Institute (ANSI) Z136.1 Class IV [4].

This ANSI standard specifies the maximum permissible exposure limit for eye-safe laser propagation, and all of these lasers would cause permanent eye damage if viewed with the naked eye at close proximity to the source.

Active satellite tracking (AST) of retroreflecting-bearing Earth-orbiters will be among the first laser propagation experiments to be performed at the OCTL. The Nd:YAG laser for these experiments is shown in Fig. 3. The laser characteristics are given in Table 2. The laser can operate in both the Q-switched and long-pulse modes at 1.064 μm, emitting 0.6 joules per pulse with a pulse repetition frequency tunable from a 1-Hz repetition rate to 51 Hz. Type-II phase-matched frequency doubling in a KD*P (deuterated potassium di-hydrogen phosphate) crystal external to the laser cavity generates 0.25 joules per pulse at 0.532 μm. AST experiments performed using both the visible and the infrared laser beams will allow an assessment of the wavelength dependence of atmospheric turbulence on laser beam propagation.

The maximum permissible eye exposure (MPE) levels and optical density (OD) needed in order to protect operators and meet Cal-OSHA requirements are given in Table 3. For the diode array, the MPEs were calculated from Eq. (1). The MPEs for the other wavelengths are given in the Society of Automotive

Table 1. Lasers for OCTL research and development projects.

Laser	Wavelength, μm	Average power, W	PRF, Hz	Energy/pulse, J	Peak power, W	Beam size at aperture, cm	Pulse width, ns
Doubled Nd:YAG [5]	0.532	12.5	1–50	0.25	0.4×10^8	30 × 21 ellipse	6.6
Yellow laser	0.589	20	CW	N/A	20	36 diameter circle	N/A
Diode array[a]	0.810	2	CW	N/A	4	9 diameter circle	N/A
Nd:YAG [5]	1.064	32	1–50	0.6	1.2×10^8	15 × 10 ellipse	8
EDFA	1.550	10	CW	N/A	20	11.8 diameter circle	N/A

[a] J. West, H. Hemmati, K. Wilson, A. Biswas, T. Roberts, M. Wright, N. Page, and D. Pieri, "Concept Design Review UAV-to-Ground Optical Communications Demonstration," JPL Presentation (internal document), Jet Propulsion Laboratory, Pasadena, California, May 3 2001.

Fig. 3. Picture of a Q-switched Nd:YAG laser beam taken by an operator using OD-6 safety goggles. The laser operates at a variety of pulse-repetition rates between 1 Hz and 51 Hz.

Table 2. OCTL Nd:YAG laser beam characteristics.

Parameter	Value	Value
Wavelength, nm	532	1064
Beam diameter at exit		
Vertical, mm	11.5	11.5
Horizontal, mm	7.4	7.4
Mean pulse width, ns	6.6	8
Standard deviation, ps	219.9	151.9
Pulse jitter, ns	2.7	2.1
Average power, W	12.8	29.7
Power stability, %, 1 s	5	6.5
Beam divergence, mrad	0.49	1.0
Polarization extinction ratio	5.8×10^{-3}	3.3×10^{-3}

Table 3. MPE and OD required for eye protection for operators of the OCTL lasers.

Laser	Average power, W	PRF	MPE, J/cm^2	OD
Doubled Nd:YAG	12.8	1	7.07×10^{-7}	6
		4	2.36×10^{-6}	5
		50	1.33×10^{-5}	5
Nd:YAG	29.7	1	1.4×10^{-6}	6
		4	4.7×10^{-6}	5
		50	2.65×10^{-5}	5
Yellow laser	20	NA	2.54×10^{-3}	4
Diode array	2	NA	1.6×10^{-3}	3
EDFA	10	NA	0.1	2

Engineers Aerospace Standard 4970 (SAE AS4970). The table gives the MPEs and ODs at a few representative pulse-repetition rates for the AST experiment laser and for the other lasers being considered for future OCTL experiments. The required eye protection specified in the table is commercially available.

The MPE for intra-beam ocular exposure for continuous-wave (CW) beams in the near-IR is given by Eq. (1) [3]:

$$MPE = C_a 10^{-2} \tag{1}$$

where

$$C_a = 10^{2(\lambda - 0.7)} \Leftrightarrow 0.7 < \lambda < 1.05 \tag{2}$$

The following series of safety procedures will be implemented at the OCTL to protect researchers and meet Cal-OSHA and JPL safety requirements. These are

(1) Shielding around the optical bench and beam path to/from the telescope.

(2) Use of safety goggles by operators of the laser system.

(3) Hazard signs posted at all entrance doors to the coudé room.

(4) A safety interlock system to preclude inadvertent entry to the OCTL coudé room during laser operation.

(5) Warning lights at entrances to the coudé room that flash when the laser is on.

(6) Use of beam dumps as terminations to optical paths.

(7) Requiring all personnel involved in laser experiments at the OCTL to have gone through laser safety training and to fulfill medical surveillance requirements.

In addition, JPL safety procedures require that the laser parameters be listed in an operation safety requirement (OSR) document and be posted at the OCTL facility.

III. Laser Beam Propagation from the OCTL into FAA-Controlled Airspace

The FAA requires operators who propagate Level-III lasers and above into the atmosphere to begin by filing a letter of intent describing the activity with the FAA. The operator then is required to determine for the specific laser operational scenario the horizontal and vertical nominal ocular hazard distance (NOHD), i.e., the slant range beyond which the laser beam irradiance becomes eye safe.

We have assessed the potential hazard posed by the lasers in Table 1 and are implementing measures at the OCTL to mitigate the risk. The design of the optical train for propagating the Nd:YAG AST laser through the OCTL telescope shows that the beams are large and elliptical at the telescope primary aperture (see Table 2). For these elliptical beams, the dimensions of the $1/e^2$ beam intensity at the telescope primary are 43 cm × 29 cm for the 0.532-μm beam, and 22.5 cm × 14.5 cm for the 1.064-μm beam. For these elliptical beams, the NOHD is given by

$$NOHD' = (2\phi)^{-1} \left\{ \left(\left(\frac{16Q}{\pi \Im(MPE)} \right) + (a_0 - b_o)^2 \right)^{1/2} - (a_o + b_o) \right\} \tag{3}$$

where

$Q =$ energy/pulse; the average power for CW beams

$\phi =$ full-angle $1/e$ beam divergence; $1/e^2$ divergence is multiplied by 0.707 to convert to $1/e$ value

$\Im(MPE) =$ MPE in J/cm^2 for pulsed lasers; MPEs in W/cm^2 for CW beams a_o and b_o are the major and minor axes of the elliptical beam

For the circular beams of the lasers of Table 4, Eq. (3) becomes Eq. (4) by substituting $a_o = b_o => D_o$ as the beam diameter at the exit aperture of the telescope:

$$NOHD = (2\phi)^{-1} \left\{ \left[\frac{16Q}{\pi \Im(MPE)} \right]^{1/2} - (2D_o) \right\} \tag{4}$$

When the beam is small enough so that $D_o << (16Q/\pi\Im(MPE)1/2$, the NOHD equation becomes

$$NOHD = \sqrt{\frac{4Q}{\pi\left(\phi^2 \Im(MPE)\right)}} \tag{5}$$

By converting centimeters to feet and radians to milliradians and evaluating $4/\pi$, Eq. (5) becomes

$$NOHD = \left(\frac{32.8}{\phi} \right) \sqrt{\frac{1.27Q}{\Im(MPE)}} \tag{6}$$

Equation (6) is the NOHD equation given by the FAA in [3].

In Table 4, we compare the NOHD using Eq. (4) for the circular beam and Eq. (6), from [3]. The results clearly show that when the beam size at the exit aperture is considered, the NOHD slant range is reduced significantly. In the case of the erbium-doped fiber amplifier (EDFA) beam, the difference is so

Table 4. Slant range of nominal ocular hazard distance for CW OCTL lasers. The 48 percent optical train transmission has been factored into these calculations.

Laser	Average power, W	MPE, W/cm^2	$1/e$ divergence, ϕ mrad	NOHD Eq. (6)	NOHD Eq. (4)	Elevation at MPE, deg
Yellow laser	20	2.54×10^{-3}	1.4×10^{-2}	42.6 km (1.4×10^5 ft)	12.2 km (3.95×10^4 ft)	16.8
Diode array	2	1.6×10^{-3}	3.5×10^{-1}	0.8 km (2.8×10^3 ft)	0.42 km (1.4×10^3 ft)	90
EDFA	10	0.1	1.4×10^{-2}	5.6 km (1.8×10^4 ft)	Eye safe at aperture	90

significant that the NOHD is reduced from 6 km to being eye safe at the aperture. In our calculations, we use Eq. (3) or Eq. (4), which better represent the laser beams propagated from the OCTL.

The elevation angle at which the laser beam becomes eye safe is also of particular significance to beam propagation through the atmosphere. For optical communications, these elevation angles will be project dependent. Yet, propagation at low elevation angles is subject to severe atmospheric turbulence effects and increased refraction and beam wander. To minimize these atmospheric effects on beam pointing, we currently have set the minimum elevation angle for beam propagation from TMF at 20 deg. The elevation angles below which the beam propagated from the OCTL would be eye safe in the atmosphere also are given in Tables 4 and 5. The optical power for the visible beams in the tables was corrected using the visual correction factor given in Table 5 of [3]. The MPEs for the IR beams were calculated using the correction factors given in Table 4 of [3].

For these calculations, we have assumed a 14-km (45-kft) aircraft service ceiling. Table 4 shows that the diode array and the EDFA beams are eye safe within the atmosphere even when propagating at zenith. The sodium laser beam is not eye safe within the atmosphere when propagating at 20 deg, our laser communication operating point, but rather at angles below 16 deg. A similar calculation was done for the AST laser using Eq. (3) for the elliptical laser beams from the Nd:YAG and doubled Nd:YAG pulsed laser beams. The results are given in Table 5 and show that, at the minimum 20-deg elevation angle, the lasers to be used in our AST experiments are not eye safe at any range in the atmosphere. To mitigate the risk posed by these lasers, JPL has defined a two-level safety system within FAA-controlled airspace, and we have developed strategies to detect aircraft and to interrupt laser beam transmission.

In addition to the NOHD, the SAE AS4970 defines three other categories for visible lasers. These are the sensitive zone exposure distance (SZED), the critical zone exposure distance (CZED), and the laser-free exposure distance (LFED), corresponding to exposure levels of 100 μW/cm^2, 5 μW/cm^2, and 50 nW/cm^2, respectively. Table 6 gives these distances for the two visible lasers listed in Table 1. These distances are calculated by substituting the respective exposure levels for the $\Im(MPE)$ term in Eqs. (3) and (4). For the 532-nm pulsed laser, the SZED (<37 m), the CZED (<177 m), and the LFED (<2 km) are all less than the NOHD. However, clearly these ranges are not a measure of the eye-safe ranges. To conform to the FAA specification, we note in Table 6 that these distances are less than the NOHD.

Because high-power laser beams will be propagated from the OCTL, our operational procedure calls for recording the OCTL telescope pointing coordinates and the date and time of beam interrupts whenever the laser beam is propagated into airspace. Data on aircraft location provided by the FAA will be recorded and archived for a period to be specified by the FAA.

Table 5. Slant range of nominal ocular hazard distance for pulsed OCTL lasers. The 48 percent optical train transmission has been factored into these calculations.

Laser	PRF	MPE, J/cm^2	Energy/pulse, J	$1/e$ divergence, ϕ mrad	NOHD Eq. (3), km	Elevation at MPE, deg
Doubled Nd:YAG	1	7.07×10^{-7}	0.25	2.1×10^{-2}	209	3.2
	4	2.36×10^{-6}	0.25	2.1×10^{-2}	230	2.7
	50	1.33×10^{-5}	0.25	2.1×10^{-2}	348	1.9
Nd:YAG	1	1.4×10^{-6}	0.6	4.1×10^{-2}	122	5.6
	4	4.7×10^{-6}	0.6	4.1×10^{-2}	149	4.5
	50	2.65×10^{-5}	0.6	4.1×10^{-2}	200	3.4

Table 6. Slant range of the SZED, CZED, and LFED for the OCTL lasers in Table 1. The 48 percent optical train transmission has been factored into these calculations.

Laser	Average power, W	SZED, km	CZED, km	LFED, km
Yellow laser	20	217	970	9700
Doubled Nd:YAG	12.5	<NOHD	<NOHD	<NOHD

A. Tier-1 Safety Strategy

The goal is to develop strategies and procedures that would support unattended remote operation of the optical communications ground stations. JPL currently is working with the FAA to define general safety measures that would support such operation. We currently are working with NASA and the San Diego traffic control (TRACON) to develop an approach acceptable to the FAA that will address the risk of illuminating aircraft in the FAA-controlled airspace, i.e., Tier 1 and Tier 2.

The Tier-1 system is designed to supplement radar coverage especially in the airspace around mountainous terrain. Around the OCTL site, low-flying and small aircraft flying in the region without transponders may be difficult to detect amidst the ground clutter from the TMF terrain. The Tier-1 system is an optical detection system that is designed to detect such craft. The system is designed to detect aircraft out to the range of 3.3 km (2 miles) and to shutter the laser before the aircraft crosses the beam. Calculations show that the 0.4-second response time of the Tier-1 system is adequate to detect and shutter the laser beam before the aircraft enters the laser beam. Tests currently are being conducted to validate the Tier-1 system performance. Beyond 3.3 km, the FAA Tier-2 radar system will detect aircraft and shutter the laser.

Aircraft at risk could be relatively fast, low-flying jets from Edwards Air Force Base (AFB) or small, slow aircraft such as a Cessna 152 at the 3.3-km (2-mile) range. In addition, the area is a favored soaring site for local sailplane pilots. The wide range of aircraft types, sizes, and speeds presents a particularly challenging "threat space" to be covered. The rapid angular rate of a jet flying above the facility at 0.3 km mandates that an effective system have a wide field of view and a rapid processing capability for detecting and identifying the aircraft in time to shutter the laser system. Also, the system must have sufficient sensitivity to reliably detect a small, dim aircraft at the 3.3-km range. Because optical communication is not limited to night operations, the system must operate both in the daytime and nighttime at angles as close as 30 deg to the Sun.

The Tier-1 system is designed around a thermal–IR detector array to meet the daytime and nighttime operations requirement. In principle, detection could be performed with a visible light camera system, assuming all aircraft use the FAA-mandated anti-collision strobe and/or wingtip navigation lights at night. However, there are instances in which a visible-light contrast reversal occurs or contrast is significantly reduced (e.g., dusk operations), such that the detection and recognition software development would be burdensome. The long wave infrared (LWIR) camera system avoids this difficulty because the target always stands out as a bright source against the dark sky, regardless of illumination conditions. The LWIR system also is expected to have more ability to observe an aircraft through moderate levels of dust and haze, conditions occasionally encountered at the TMF site, through which communications and laser experiments are expected to continue. Finally, the LWIR system has the advantage of not requiring aircraft lighting for detection at night, an added safety feature.

A picture of the Tier-1 system is given in Fig. 4. To enhance the certainty of detecting all aircraft within the exclusion region, it includes a pair of LWIR cameras based on the Raytheon Control IR 2000B barium strontium titanate (BST) focal plane array. Each array has a reported noise equivalent temperature difference (NETD) of 130 mK and is comprised of 320×240 active pixels. One of the cameras uses an F/1.0 75-mm germanium lens to generate a 12×9 deg field of view with heightened sensitivity to see small aircraft at the full 3.3-km (2-mile) design range. The other uses an F/1.0 18-mm germanium lens for a 46×35 deg field for identifying rapid, low-flying aircraft at high angles before they encounter the beam. Both cameras are aimed at the same point in the far field, and the system is to be mounted to the telescope structure, bore-sighted to the center of the telescope field of view (FOV).

Sensitivity of the camera system becomes an issue when working with the 18-mm lens, however. The BST camera engine uses an auto-scaling algorithm to set the system offset and gain. With the wide field-of-view (WFOV) lens, the shorter targets at range significantly under fill a pixel. Since each pixel has such a large footprint on the sky, the collected background is very high, limiting the total signal-to-noise ratio of the sensor. Furthermore, each pixel's gain is partially set by the flux incident on neighboring pixels, so nearby bright objects will cause a significant sensitivity reduction on a pixel, even if that pixel is not directly exposed to the source. This is the so-called halo effect. The net effect is that a lens with

Fig. 4. Image Labs International Tier-1 aircraft avoidance system consists of two LWIR cameras (a wide field of 35 deg×46 deg and a narrow field of 12 deg×9 deg).

a longer focal length will be much more effective at limiting the background noise on a pixel and will spatially narrow the halo region, significantly improving the system's sensitivity in the region around the beam.

The Image Labs International (ILI) system software performs two sets of algorithms to ensure that targets are not overlooked, but also to minimize the number of false alarms. Because its field of view is so wide (up to 45 deg) the 18-mm camera system is expected to see many "fixed" objects near the communication telescope (e.g., trees and mountains near or on the horizon, or bright cumulus clouds separated by dozens of degrees from the beam). To prevent these bright, fixed objects from triggering the shutter, a temporal filter is used to look for changes in the WFOV scene. Since the aircraft are assumed to move with respect to the static scene, the filter enhances the motion, allowing the target to stand out against the relatively bright objects in the background. Once an aircraft is identified, it is tracked to determine its potential to intercept the beam. If the track comes sufficiently close to the beam, the algorithm interrupts the "all clear" signal, causing the shutter to close. Some anticipated operational scenarios include lasing while the telescope is slewing to track an object such as an aircraft or low-Earth-orbit (LEO) satellite. In this case, the telescope transmits slewing information to the aircraft-spotting system computer, and the background image is offset by the angular slew rate. A moving aircraft still stands out in the tests performed, validating the approach.

To identify fast-moving targets quickly, a quick identification algorithm runs concurrently and also has the ability to shutter the beam. In this case, when a bright object of sufficient size is detected sufficiently close to the beam, the shutter closes. This algorithm is activated by very fast or very low-flying objects. In addition, the algorithm will shutter the laser in the event that any object, such as a dark cloud, comes sufficiently close to the beam that it could be obscuring an aircraft that might rapidly emerge from behind it.

As a fail-safe design, the normal state of the system is to have the laser transmission blocked. Both cameras and both target identification algorithms must be operational and must provide an "all clear" signal to keep the shutter open. Under this condition, the laser beam will be allowed to propagate.

The Tier-1 software allows for modification of all of the target detection and identification parameters, as well as the parameters at shut down. This allows the operator to determine the optimal operating conditions and to minimize the false-alarm rate while maintaining a safe operational system. The operator has access to the operational information through the real-time display, which shows the raw images generated on both camera systems, and color-coded tracking information allows the operator to understand which algorithms are running and which ones are triggered by various objects within the field of view.

B. Tier-2 Safety Strategy

The FAA monitors all U.S. air-controlled civilian airspace and can under certain conditions make this information available to NASA and other government agencies. Safe laser beam propagation through Tier 2 from AMOS is achieved using the radar display interface (RDI) system [6]. The system takes a radar feed from a traffic control (TRACON) center and displays the location of aircraft superimposed on a local topographic map. The feed is unidirectional, so that the end user only receives data from the FAA and cannot transmit data back into the system.

A typical display screen from the AMOS RDI system is shown in Fig. 5. Aircraft are shown as dots, and the pointing direction of the laser beam is shown as a line with an exclusion zone shown as a triangle. This display reports on the status of the RF link between AMOS and the FAA TRACON. The plan for TMF operations is that aircraft detections by the FAA's Long Beach and Boron radar facilities will be relayed to San Diego TRACON, at which point the OCTL will access the data.

Fig. 5. The RDI system developed by Boeing Technical Services for the AMOS. The system shows aircraft positions superimposed on a topographic map of the Hawaiian Islands. The display reports on the RF link to the FAA (up). The exclusion zone, the laser-beam pointing direction, and the location of a detected aircraft (red dot) also are shown. The laser uplink is off. The picture is courtesy of Capt. J. Snodgrass, Maui Space Surveillance Center, U.S. Air Force.

NASA has been discussing upgrading the RDI approach for implementation at the OCTL. The upgrade will address certain key features desired by the FAA. These are to

(1) Define a conical rather than triangular exclusion zone to better reflect the threat posed by the laser beam. An aircraft traversing the beam's azimuth pointing direction is not necessarily at risk if its elevation is different from that of the beam.

(2) Display an icon to confirm that the computer system is operating during updates of the aircraft location display.

(3) Display a tracking icon to indicate the direction of motion of an aircraft.

NASA and the FAA are exploring the preparation of a joint memorandum of agreement (MOA) to address the Tier-2 needs identified by the FAA. If the FAA accepts the RDI system as the approach for remote autonomous operation, the three key areas that will be covered by the MOA are to

(1) Define the interface to the FAA's radar system.

(2) Specify a maximum delay for access to the aircraft data. This will be critical to defining the exclusion zone.

(3) Handle, distribute, and archive radar display data.

1. Tier-2 Safety Strategy Used in Past Demonstrations. The use of a bore-sighted weather radar to detect aircraft at risk was approved by the FAA during the 1996 and 1997 Ground/Orbiter Lasercomm Demonstration (GOLD). The Honeywell Primus-40 WXD radar shown in Fig. 6 provided Tier-2-level safety. The system has a maximum range of approximately 500 km, and its parameters are given in Table 7 [7].

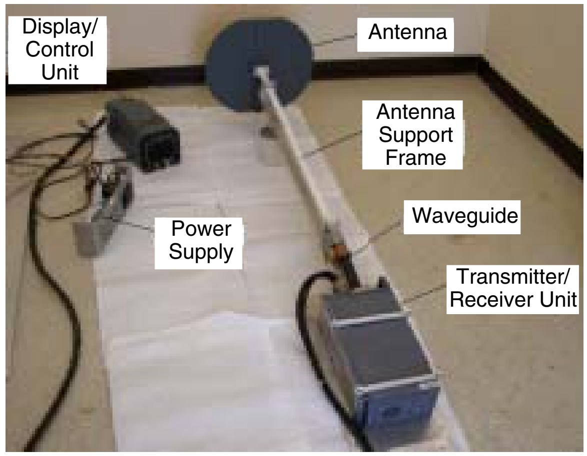

Fig. 6. Honeywell Primus-40 weather radar (used for aircraft detection during the 1996 GOLD optical communications demonstration).

Table 7. Primus-40 radar system parameters.

Parameter	Value
Average power	3 W
Peak power	7 kW
Pulse width	1 μs
Repetition rate	121 Hz
Operating frequency	9345 MHz
Bandwidth	375 kHz
Antenna diameter	0.45 m
Minimum detectable signal	−108 dBm

Using the radar parameters in Table 7 with the following radar equation, one can estimate the system's capability to detect aircraft [8]:

$$R_{\max} = \left[\frac{P_T G A_e \sigma}{(4\pi)^2 S_{\min}} \right]^{1/4} \tag{7}$$

where P_T is the power transmitted, G is the transmitter antenna gain, A_e is the effective receiver area, σ is the target cross section, and $S_{\min}$ is the minimum detectable signal. The radar cross section is a function of the radar wavelength and the aspect angle of the target with respect to the incident beam. Reference [9] gives nominal cross sections at microwave frequencies for various objects at normal incidence. These are 1 m^2 for a small, single-engine craft, 40 m^2 for a large jet airliner, and 100 m^2 for a large jumbo jet. Because the cross section varies with aspect angle, the radar return signal also will vary with aspect angle. Yet, although these cross sections will differ with aircraft, these cross sections do provide a guideline for bounding the applicability of this radar to aircraft detection. Using the cross sections above and the data from Table 7 in Eq. (7), we calculate the maximum ranges for these targets to be 26 km, 65 km, and 82-km, respectively.

Estimating the mean sea-level service ceilings of these aircraft at 7.6 km (20 kft), 12.2 km (40 kft), and 13.7 km (45 kft), respectively, these aircraft altitudes correspond to elevations of 12.5, 9, and 8 deg from the 2.2-km-altitude OCTL ground station, elevations that are well below the 20-deg minimum-operation elevation for beam propagation from the OCTL. With the 20-deg minimum-elevation operational constraint, the ranges to these aircraft when operating at their service ceilings are 15 km, 29 km, and 34 km, respectively. The estimated radar returns for the three types of aircraft are correspondingly 9, 14, and 15 dB above the minimum detectable signal, $S_{\min}$. For the GOLD project, the Honeywell radar was tested on aircraft out to approximately 25 km. The Primus-40's systems electronics were modified so that the return radar signal generated a transistor–transistor logic (TTL) trigger that activated a laser beam interrupt whenever an at-risk aircraft was detected. The electronic system for laser-shutter trigger and radar-system diagnostics signals uses receive and transmit TTL signals from the display unit, respectively. The TTL signal from transmit is positive-going 12-V square wave at 121 Hz, and the receive signal is +4.5 V square wave at the same frequency in the presence of a target in the radar field. Figure 7 shows an oscilloscope displaying these signals.

Each signal is fed through a comparator that is held at a +3.3-VDC reference voltage through a voltage divider biased at +5 VDC. The output signal from the comparator is fed to a dual monostable multivibrator (MMV) biased at +5 VDC and switches the trigger signal for the laser shutter controller. When the radar unit is on and there is a target present, the transmit and receive TTL signals trigger the comparators to send a negative-going pulse to the input of the MMV, hence invoking the +5 VDC trigger signal for the laser-shutter controller. Figure 8 is a schematic diagram for the electronic system.

Frequency allocation and coordination with other radiating facilities are critical when operating at these radio frequencies. JPL coordinated its radar transmission with Ft. Irwin and has the following frequency assignments at TMF: 9375-MHz frequency, 50-kW power, and 5-MHz bandwidth; and 9344-MHz frequency, 3-W power, and 375-kHz bandwidth.

An on-site radar system is a general approach to ensuring safe laser beam propagation from autonomously operating ground stations in locales not covered by FAA or other radar systems. Autonomous operation is constrained by the FAA requirement to have outside observers to shutter the laser beam should there be an identified risk. In the absence of a Tier-1 system, the use of an on-site radar system still requires the use of outside observers. We plan to evaluate the Tier-1 system and to seek FAA approval for its use as an alternative to the outside observer.

As we develop the RDI system, we plan to use the Primus-40 weather radar system for achieving safe beam propagation in the Tier-2 region. Commercially, Honeywell has developed a laser hazard reduction system (LHRS) that uses radar for aircraft avoidance [9]. This system consists of a rotating antenna in a protective dome, and it has been integrated with several satellite laser-ranging stations to ensure safe

Fig. 7. Transmit and receive signals from the display unit.

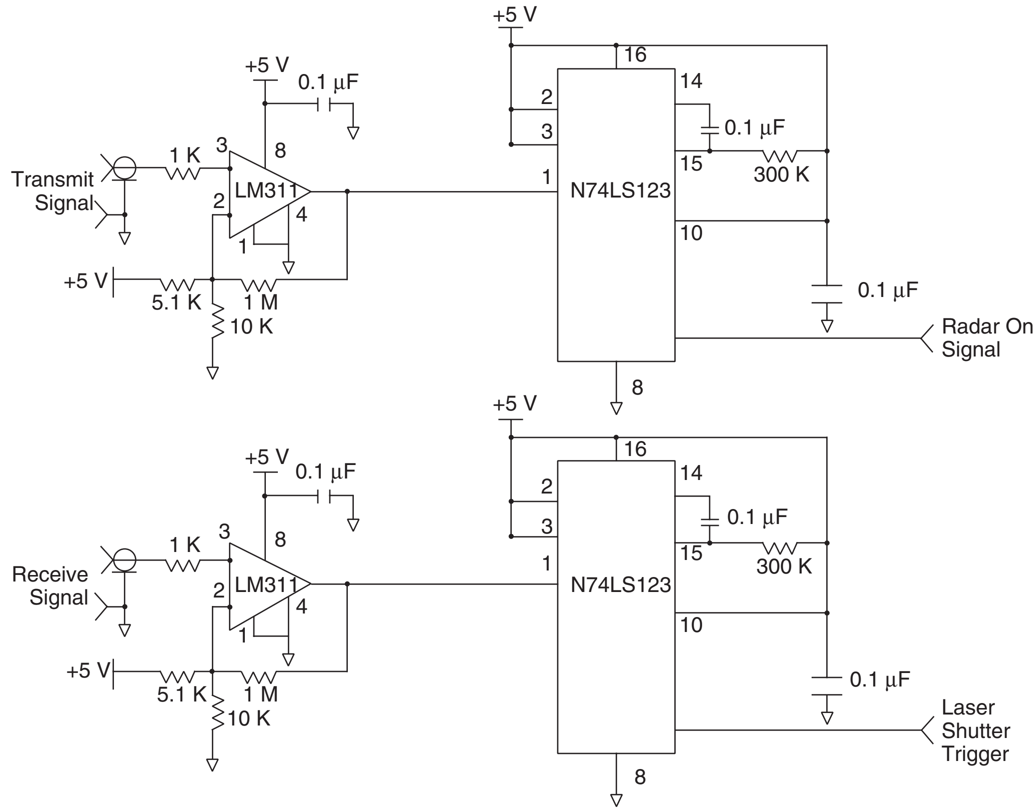

Fig. 8. Schematic diagram of Tier-2 electronics.

laser beam propagation. To protect the sensitive receiver electronics from reflections from the outgoing radar signal, the receiver has a main bang suppressor that precludes detection of aircraft at closer than 200 m.

There are Cal-OSHA safety stipulations for safe operation of radar systems such as the Primus-40. The requirement is that personnel be no closer than 1.8 m from the antenna during operation [7]. This requirement will be readily met during OCTL operations since the radar will be attached to and be bore sighted with the telescope, and it will be turned on only when the dome slit is open and the telescope is pointed out through the open dome slit.

IV. Tier-3 Safety System

The Tier-3 safety layer is the predictive avoidance to prevent inadvertent illumination of either U.S. or foreign satellites. Safe laser beam propagation from the U.S. into space requires that the laser and its site be registered with the U.S. Space Command. The registration information includes

(1) Specification of the peak and average laser outputs.

(2) Laser site location.

(3) Laser wavelength.

(4) Laser track across the sky and for the duration of propagation.

In addition, the Clearinghouse now requires that operators present proof that they are authorized to illuminate their target satellites. Based on the laser propagation details, the Laser Clearinghouse can either issue a blanket approval of transmission at the time of registration or require coordination of all laser beam propagation activity.

Table 8 gives the laser characteristics for three ground-to-space laser communication demonstrations conducted from JPL's TMF. For some of these demonstrations, such as GOLD and Space Technology Research Vehicle-2 (STRV-2), JPL received blanket approval [10,11]. For these demonstrations, a data stream was impressed on CW lasers. This was very different from the modulation used in the deep-space Galileo Optical Experiment (GOPEX) demonstration. The lasers transmitted from the Starlight Optical Range (SOR) and from TMF were Q-switched Nd:YAG lasers with peak powers of 20 MW and 23 MW, respectively [12]. It was deemed that these high peak-power levels could affect sensitive satellite sensors, and laser beam transmissions had to be coordinated with the Laser Clearinghouse.

In the case of unattended remote operation that requires coordination, Tier-3 safety will be implemented by programming the laser shutter to interrupt the laser beam at those times that the Laser Clearinghouse has precluded transmission.

Table 8. GOPEX laser transmitter characteristics.

Project	Transmitter characteristic			Predictive avoidance
	Parameter	TMF	SOR	
GOLD				No
	Wavelength, nm	514.5	—	
	Laser power, W	7.5	—	
	Beam divergence, μrad	30	—	
STRV-2				No
	Wavelength, nm	810, 852	—	
	Laser power, W	0.75, 0.54	—	
	Beam divergence, μrad	40, 400	—	
GOPEX				Yes
	Wavelength, nm	532	532	
	Pulse energy, mJ	250	350	
	Repetition rate, Hz	15–30	10	
	Pulse width, ns	12	15	
	Beam divergence, μrad			
	Days 1–4	110	80	
	Days 6–8	60	40	

V. Summary

Lasers will be used to support future high-bandwidth space-to-ground communications from NASA's deep-space probes. The use of high-power lasers to communicate with deep-space probes will require implementing safety strategies to ensure that neither aircraft nor satellites are illuminated by the laser beams. We have described a strategy for safe laser beam propagation from ground stations to NASA's deep-space probes. The strategies address safety concerns of Cal-OSHA, the FAA, and the Laser Clearinghouse, the government agencies with responsibilities related to laser operation and laser beam propagation. We plan to implement this approach at the JPL's OCTL facility and to work with the appropriate regulatory agencies to have the OCTL experiments serve as a precursor to developing a safe laser beam propagation strategy that will support remote autonomous operation of a future high-bandwidth optical deep-space network.

Acknowledgments

The authors would like to thank L. Tonish (FAA Airspace Branch AWP520.1) and J. Tomlinson (AWP520-Airspace Project Office, FAA), who continue to work with us to develop the operational specifications of the RDI system, and Captain J. Snodgrass of the U.S. Air Force Maui Optical Station for his assistance and collaboration as we continue to define the RDI system.

References

[1] W. J. Weber, R. B. Miller, P. E. Doms, and R. Cesarone, "A View of the Future of NASA's Deep Space Network and Associated Systems," to be published in *Proceedings of SpaceOps Conference,* Houston, Texas, October 2002.

[2] K. E. Wilson, M. Britcliffe, and N. Golshan, "Recent Developments in the Construction of the Optical Communications Telescope Laboratory," *SPIE Free-Space Laser Communication Technologies Proceedings,* vol. 3932, San Jose, California, January 2000.

[3] U.S. Department of Transportation, Federal Aviation Administration, AC No: 70-3, "Outdoor Laser Operation(s)."

[4] *The Laser Institute of American National Standards for Safe Use of Lasers Outdoors ANSI Z 136.6,* Appendix B, p. 71, February 15, 2000.

[5] K. Wilson, "Planned Operations for the JPL Optical Communications Telescope Laboratory (OCTL)," Invited Paper, CRL International Symposium on Light Propagation and Sensing Technologies for Future Applications, Tokyo Japan, March 2002.

[6] J. Snodgrass, "Maui Space Surveillance Complex (MSSC) FAA Radar Display System," Air Force Research Laboratory (AFRL) and Boeing briefing to the FAA, Maui, Hawaii, June 15, 2001.

[7] RCA, *Primus-40 WXD Service Manual IB8029050,* Rev. 3, p. 4-3, October 1978.

[8] M. Skolnik, *Introduction to Radar Systems,* Second Ed., New York: McGraw-Hill p. 15, 1980.

[9] Honeywell Corporation, "Laser Hazard Reduction System and Laser Interlock Overview," Technical Note, August 2001.

[10] K. Wilson, M. Jeganathan, J. R. Lesh, J. James, and G. Xu, "Results from Phase-1 and Phase-2 GOLD Experiments," *The Telecommunications and Data Acquisition Progress Report 42-128, October–December 1996,* Jet Propulsion Laboratory, Pasadena, California, pp. 1–11, February 15, 1997. http://tmo.jpl.nasa.gov/tmo/progress_report/42-128/128K.pdf

[11] K. E. Wilson, E. Korevaar, J. Ceniceros, M. Wright, N. Page, J. Kenny, and P. Moynihan, "Plans for a STRV-2 to AMOS High Data Rate Bi-Directional Optical Communications Link," AMOS Technical Conference, Maui, Hawaii, September 1999.

[12] K. E. Wilson and J. R. Lesh, "An Overview of the Galileo Optical Experiment (GOPEX)," *The Telecommunications and Data Acquisition Progress Report 42-114, April–June 1993,* Jet Propulsion Laboratory, Pasadena, California, pp. 192–204, August 15, 1993. http://tmo.jpl.nasa.gov/tmo/progress_report/42-114/114Q.pdf